Mine Closure 2023 - Behrooz Abbasi, Jeff Parshley, Andy Fourie & Mark Tibbett (eds)

doi:10.36487/ACG_repo/2315_094

Valorisation of mine waste as carbon mineralisation feedstock

EW Gazzetti *MineraLogic, USA*

JZ Bandstra *MineraLogic, USA*

TR Diedrich *MineraLogic, USA*

Abstract

Growing incentives to decarbonise the economy are creating new opportunities for valorising mine waste. One of these emerging opportunities involves carbon sequestration via carbon mineralisation using mine waste with amenable chemistry as mineral feedstock. At earth's surface, the process of converting atmospheric CO_2 into stable mineral phases occurs naturally—and slowly—over geologic time scales. Mine waste presents a unique opportunity for enhanced carbon mineralisation due to large quantities of freshly exposed reactive surface area created by blasting, crushing, and other beneficiation processes. To date, most surficial carbon mineralisation demonstrations have targeted the mineral brucite, a mechanism that applies to less than 5% of mine waste types. Unlocking potential from the remaining 95% on human timescales requires site-by-site geochemical evaluations of waste material and subsequent development of waste management strategies designed to optimize carbon mineralisation.

A geochemical modelling-based program has been developed and applied to rapidly assess the carbon mineralisation potential of a wide range of mine waste compositions. This program uses data routinely obtained through standard geochemical analyses. Modal mineralogy, bulk elemental compositions, and either site-specific (e.g., derived from bench-scale tests) or literature-based reaction rates are used to predict carbon mineralisation rates using a geochemical model operating in a batch-reactor configuration. The ability to opportunistically use data that many mines already have available allows for materials to be rapidly screened (and, if applicable, ranked) for carbon mineralisation potential prior to engaging in costly specialized programs.

Initial applications of this model indicated that passive mineral carbonation rates—i.e., mineralisation occurring under routine conditions of mine waste management—at North American mine sites range up to approximately 0.44 kg CO_2 per tonne of waste material per year. When scaled up to typical masses of mine waste management features, mineralisation can be appreciable. Furthermore, the geochemical model indicates that these rates can be improved substantially through mine waste management practices that are likely to enhance kinetics, including hydrological controls, grain size optimizations, and the introduction of heat. Outstanding themes requiring refinement to advance state-of-the-art practices in carbon mineralisation include (i) scaling factors to improve suitability of literature-based kinetics in modelling efforts, (ii) changes to mineral reactivity with time, and (iii) verification/quantification methods at bench, pilot, and field scales.

Keywords: *decarbonise, sequestration, mineralisation, carbonation, valorisation*

1 Introduction

As a source of both (future) materials needed for electrification and (historically) significant carbon emissions, the mining industry can make a critically important contribution to global efforts to decarbonize the economy. Mining companies have been notably responsive to this opportunity by setting aggressive internal net-zero greenhouse gas (GHG) emissions goals. As of 2021, 21 of the 30 largest metals mining companies had net-zero GHG emissions goals with target dates of 2050 or sooner (Kuykendall, 2021). Additional companies have since pledged to net-zero goals by 2050 as part of their membership with the International Council on Mining and Metals (ICMM; (IFC, 2023).

Meeting these goals while satisfying a growing metals demand will require complementary sets of strategies to reduce *and* offset emissions. For example, for copper and nickel mining, it has been estimated that

approximately 90% of the industry's progress toward net-zero will likely come from emissions reductions (IFC, 2023)—resulting from actions such as improving efficiency, expanding use of renewable energy and "green" fuels, and fleet electrification. Offsetting the remaining 10% is expected to include some form of long-term carbon sequestration strategy. Reforestation projects and other nature-based solutions are mature and can represent relatively inexpensive offset opportunities; however, they require maintenance and can be ephemeral (IFC, 2023). A viable and emerging alternative for offsetting emissions is sequestration of carbon in the form of stable carbonate minerals (i.e., "carbon mineralisation") via enhanced rock weathering.

1.1 Carbon mineralisation geochemistry

Carbon mineralisation, or the conversion of atmospheric CO_2 into stable mineral phases, happens naturally at earth's surface. Carbonate rocks comprise a huge reservoir of carbon (roughly 87% of the total carbon mass on Earth), and the chemical reactions leading to their formation are well established. For example, the geochemical process by which chemical weathering consumes CO_2 is exemplified below by the dissolution of anorthite ($CaAl_2Si_2O_8$) and precipitation of calcite ($CaCO_3$):

$$2 \cdot CO_2 + 3 \cdot H_2O + CaAl_2Si_2O_{8(s)} \rightleftharpoons Ca^{2+} + 2 \cdot HCO_3^- + Al_2Si_2O_5(OH)_{4(s)} \quad (1)$$

$$Ca^{2+} + 2 \cdot HCO_3^- \rightleftharpoons CaCO_{3(s)} + CO_2 + H_2O \quad (2)$$

In reaction (1), anorthite undergoes hydrolysis, releasing divalent calcium cations (Ca^{2+}) to solution and converting dissolved CO_2 to bicarbonate ions (HCO_3^-). In reaction (2), calcite precipitation consumes one of the bicarbonate ions formed in reaction (1). When these reactions occur in a solution that is open to the atmosphere, reaction (1) draws CO_2 into solution and reaction (2) locks it up in a geologically stable solid. Analogous reactions occur which invoke dissolution of magnesium-bearing phases and precipitation of magnesium carbonates.

However, the typical reactions that convert atmospheric CO_2 into mineralised carbon in geologic contexts occur slowly. Activities related to mining tend to promote the overall magnitude and efficiency of carbon mineralisation by isolating materials with enhanced reactivity (due to their mineralogy and/or abundance of reactive surface area) and creating conditions that are favourable for carbon mineralisation (Power et al., 2013; Renforth, 2019).

1.2 Mine waste and carbon mineralisation

Non-ore grade rock and residues from ore processing (collectively referred to here, as "mine waste") have been shown in field and laboratory trials to mineralize carbon from reaction with atmospheric or point-source CO_2. Select examples of carbon mineralisation projects which use mine waste as feedstock are provided in Table 1. While not exhaustive, these examples illustrate the variety of material types and project designs which have been utilized or tested for this purpose.

Most of the field demonstrations indicated in Table 1—and the published literature germane to carbon mineralisation associated with mining activities—target the mineral, brucite. This magnesium-hydroxide, while not a common rock forming mineral, can be found in specific geologic environments, including serpentinized ultramafic intrusions and chrysotile deposits. Annual production of tailings from these types of deposits makes up considerably less than 5% of total annual tailings production (calculated from Supplementary Information 2 from (Bullock et al., 2021)). Brucite is highly reactive and will readily sequester carbon if exposed to atmospheric CO_2. However, as indicated in Table 1, carbon mineralisation opportunities exist beyond brucite, and there are a (growing) number of engineered approaches that can be applied to enhance carbon mineralisation rates in the field. Identifying reactive silicate minerals, the largest class of minerals on earth, as feedstock for carbon mineralisation has the potential to identify carbon mineralisation opportunities, with or without engineering advances, at many mine sites.

Table 1. Breadth of demonstrated carbon mineralisation opportunities

Primary Mineral Reactants	Geologic Context	Description of Demonstration	Reported Carbon Sequestration Rates
Brucite (Mg)	Serpentinized ultramafic mine waste associated with magmatic nickel deposits	**Dumont Nickel Project** *(Passive mineralisation of tailings in field cells)*	1.4 kg CO_2/tonnes tailings/y [(1)]
		Mt. Keith Mine *(Passive mineralisation in full-scale tailings facility)*	2.4 kg CO_2/m^2 facility surface/y [(2)]
		Baptiste nickel deposit *(Tests representing passive reaction of tailings with atmosphere)*	Initially 3.5 kg CO_2/m^2 facility surface/y before decreasing [(3)]
		Baptiste nickel deposit *(Simulation of tailings in atmosphere with active aeration)*	19 kg CO_2/m^2 facility surface/y [(3)]
		Baptiste nickel deposit *(Laboratory testing with CO_2-rich gases)*	0.07 to 0.14 %C/hour [(3)]
	Chrysotile mine wastes	**Woodsreef Mine** *(Passive mineralisation at tailings facility)*	12 kg CO_2/m^2 facility surface/y [(4)]
		Thetford Mines *(Passive mineralisation of milling waste field cells)*	Approx. 19 kg CO_2/m^2 facility surface/y [(5)]
Magnesium Silicates (serpentine, olivine, pyroxene) in absence of brucite	Kimberlite	**Diavik Mine** *(Passive mineralisation in processed kimberlite facility)*	Approx. 0.4 kg CO_2/m^2 facility surface/y [(6)]
	Fe-rich silicate residue from an apatite mine	**Mine Arnaud** *(Lab tests of ex situ mineralisation with flue gas CO2 and iron complexation via a chelating ligand)*	130 kg CO_2/tonne residue [(7)]
	Slag produced from lateritic ores	**New Caledonia nickel mines** *(Laboratory testing under elevated temperature and CO_2 conditions)*	Not Reported [(8)]
Calcium Silicates (anorthite, calcium-rich pyroxene)	Magmatic Ni-Cu ± PGE	**Stillwater Mine** *(Tests representing carbon mineralisation of tailings at ambient temperatures and pressures with elevated CO_2)*	1.79 kg CO_2/tonne tailings [(9)]
		Duluth Complex *(Tests and simulation representing passive mineralisation of mine waste)*	0.44 kg CO_2/tonne material/y)[10]

[1] Gras et al. (2020); [2] Wilson et al. (2014); [3] Power et al. (2020); [4] Hamilton et al. (2021), study also assessed effect of heap leaching with acidic solution and water, which did not have a notable effect on mineralisation rates; [5]Lechat et al. (2016), assumes field cell has surface area of 81 m^2 ; [6] Wilson et al. (2011); [7] Reynes et al. (2021); [8] Kularatne et al. (2023); [9] Woodall et al. (2021) [10]Bandstra et al. (In prep.)

1.3 Identifying mine waste for use as carbon mineralisation feedstock

A geochemical modelling-based program has been developed and deployed to rapidly identify the carbon mineralisation potential of materials on mine sites. This program opportunistically utilizes data that are often collected for other purposes, including exploration and waste characterization, with the goal of expanding the types and amounts of mine waste that can be used as feedstock in carbon mineralisation programs. The carbon mineralisation evaluation is conducted in three stages:

1. Screening for bulk carbon mineralisation potential.
2. Kinetic modelling of carbon mineralisation rates.
3. Evaluation of potential carbon mineralisation rate enhancement.

1.3.1 Screening for bulk carbon mineralisation potential

Bulk carbon mineralisation potential (C_{pot}) describes a material's capacity to mineralize carbon in the form of carbonate minerals. It represents the maximum amount of CO_2 that can be consumed with the complete reaction (i.e., dissolution) of a solid material. Potential is constrained by bulk mineralogy, specifically the elemental compositions of calcium, magnesium, sulphur, phosphorus, and carbon. Materials with relatively high calcium and magnesium concentrations, relatively low sulphur and phosphorous concentrations, and limited amounts of pre-existing carbonate minerals have the most potential.

This screening calculation is a rapid and transparent step toward assessing carbon-related opportunities. Data requirements are minimal and often coincide with other project needs. Results are used to qualitatively rank materials and to identify targets for additional analyses. For demonstration purposes, publicly available geochemistry data from the United States Geological Survey (USGS) Earth Mapping Resources Initiative (Earth MRI) were screened for carbon mineralisation potential. Earth MRI aims to identify areas that may contain undiscovered critical minerals. Its geochemistry dataset ranges across the United States, creating an opportunity to rapidly assess a large sample of lithologies.

1.3.2 Kinetic modelling of carbon mineralisation rates

Though silicate minerals have considerable potential, their suitability as feedstock for carbon mineralisation is rate limited. Theoretically, a material could possess "high potential" but the release of calcium and magnesium—the cations necessary for mineralisation—is so slow that measuring sequestration is impractical on a human timescale. Kinetic modelling evaluations, as described in Section 2.2, incorporate literature-based or site-specific rate data to constrain timescales associated with cation dissolution (i.e., release) and carbonate precipitation. Kinetic modelling also allows for the evaluation of site conditions such as pH that may inhibit or enhance carbon mineralisation reactions.

When available, site-specific rate data produce more favourable and, potentially, more realistic carbon mineralisation results than literature-based rate data. Published rate data, which are based on experiments involving mineral separates, can vary across sources, and are relatively limited in their applicability to multi-phase aggregates (i.e., rocks). Site-specific rate data, derived from kinetic test (e.g., barrel, humidity cell, or column) results, offer a comprehensive picture of the kinetics observed on actual project rocks. The authors observed a roughly 3x increase in predicted carbon mineralisation rates when site-specific rate data are used. Nevertheless, literature-based rate data are convenient (kinetic test results are not always available) and provide reasonable, if not conservative, mineralisation predictions appropriate for a desktop evaluation.

1.3.3 Evaluation of potential carbon mineralisation enhancements

Modifications of the geochemical modelling evaluation are conducted to assess the efficacy of targeted carbon mineralisation rate enhancements. Potential scalable enhancements include hydrological controls, grain size optimizations, introduction of heat, and variable partial pressure of CO_2 (P_{CO_2}).

2 Methodology

For illustrative purposes, the geochemical program to identify carbon mineralisation potential that is described above was applied to published or otherwise available data.

2.1 Carbon mineralisation potential

Bulk C_{pot} estimates were based on a modified version of the Steinour formula (Renforth, 2019; Steinour, 1959):

$$C_{pot} = \frac{M_{CO_2}}{100} \cdot \left(\boldsymbol{\alpha} \frac{\mathrm{CaO}}{M_{\mathrm{CaO}}} + \boldsymbol{\beta} \frac{\mathrm{MgO}}{M_{\mathrm{MgO}}} + \boldsymbol{\gamma} \frac{SO_3}{M_{SO_2}} + \boldsymbol{\delta} \frac{P_2O_5}{M_{P_2O_5}} \right) \cdot 10^3 \quad (3)$$

where CaO, MgO, SO_3, and P_2O_5 are elemental compositions in weight percent of calcium, magnesium, sulphur, and phosphorous, respectively, and M_x is the respective molar mass of the associated oxide. Equation (3) acts as a ledger of carbon mineralisation potential by summing these elements' ability to contribute to or detract from carbon sequestration. Coefficients α and β are positive (+1), while γ and δ are negative (-1 and -2, respectively). As a result, calcium and magnesium improve carbon mineralisation potential, while phosphorous and sulphur depress it.

Primary silicate minerals generally show reasonable carbon mineralisation potential that becomes significant when scaled to mine waste masses typically observed at mine sites (Table 2).

Table 2 Carbon removal capacity of common silicate minerals expressed in terms of carbon mineralisation potential (C_{pot})

Name	Chemical Formula	Mineral Group	C_{pot} (kg CO_2/tonne)
Forsterite	Mg_2SiO_4	Olivine	626
Fayalite	Fe_2SiO_4	Olivine	0
Chrysolite	$Mg_{1.8}Fe_{0.2}SiO_4$	Olivine	539
Enstatite	$MgSiO_3$	Pyroxene	438
Orthoferrosilite	$FeSiO_3$	Pyroxene	0
Diopside	$CaMgSi_2O_6$	Pyroxene	406
Tremolite	$Ca_2Mg_5Si_8O_{22}(OH)_2$	Amphibole	379
Actinolite	$Ca_2Mg_4FeSi_8O_{22}(OH)_2$	Amphibole	313
Hornblende	$NaCa_2Mg_5Fe_2AlSi_7O_{22}(OH)$	Amphibole	332
Muscovite	$K_2(Si_6Al_2)Al_4O_{20}(OH)_4$	Mica	0
Biotite	$K_2(Si_6Al_2)Mg_4Fe_2O_{20}(OH)_4$	Mica	196
Phlogopite	$K_2(Si_6Al_2)Mg_6O_{20}(OH)_4$	Mica	316
Orthoclase	$KAlSi_3O_8$	Feldspar	0
Albite	$NaAlSi_3O_8$	Feldspar	0
Anorthite	$CaAl_2Si_2O_8$	Feldspar	158
Quartz	SiO_2	Silica	0

Geochemistry data were extracted from the USGS Earth MRI website. Elemental compositions measured using Inductively Coupled Plasma Mass Spectroscopy (ICP-MS) were fed into Equation (3) via an automated Python script to enable rapid and systematic processing of data across all Earth MRI Projects included in the evaluation.

Data fields from the Earth MRI geochemistry dataset that were used in this evaluation include project name as defined by USGS (e.g., Hicks Dome area -southeastern Illinois), sample type, and analytical method; the dataset was filtered to focus on rock samples analysed using ICP-MS. In total, 25 Earth MRI projects met our requirements. Some projects were combined based on deposit similarities (e.g., “Hicks Dome area – southeastern Illinois” and “Hicks Dome area – Kentucky” were combined into “Hicks Dome area – IL and KY”). This reduced the number of projects in this evaluation to 21.

Equation (3) assumes that all calcium and magnesium present in the bulk material represents the potential to mineralize additional CO_2 (i.e., it does not reflect the presence of calcium and magnesium already present as carbonate minerals). Therefore, unless corrected, the formula tends to overestimate bulk carbon mineralisation potential of materials with significant carbonate content. Carbon concentrations were unavailable in the Earth MRI geochemistry dataset, making it impossible to quantitatively correct for pre-existing carbonate minerals. To account for this deficiency, several “rock names”, as identified by USGS, were removed from the evaluation based on a qualitative assumption of high carbonate content (e.g., “carbonate”, “dolostone”, and “marble”). Theoretically, the remaining samples should have minimal inorganic carbon concentrations.

2.2 Carbon mineralisation rates and enhancements

Carbon mineralisation rates were simulated in PHREEQC (Parkhurst and Appelo, 2013) with primary minerals as kinetic reactants and secondary precipitates treated as equilibrium phases. All simulations assumed well-mixed batch behaviour with fixed temperature and equilibrium of dissolved gasses with a constant atmosphere. Mineral dissolution kinetics were derived from peer-reviewed rate compilations as described below. Dissolution rates are taken at far-from-equilibrium values to represent the leaching of material from the mineral surface rather than long-term steady-state hydrolysis of the crystal framework.

In long-term simulations (> 10 years), kinetic reactants were depleted according to the shrinking particle model (Rimstidt, 2014). In this way, our results may be viewed as an extension of kinetic modelling reported in Bullock et al. (2021). In short-term simulations (< 10 years), shrinking particle effects were found to be negligible and were neglected in the results reported.

PHREEQC simulations were automated via python script using the IPHREEQC COM (Charlton and Parkhurst, 2011). Automation enabled systematic simulation of conditions for potential enhancement of carbon mineralisation rates including sulphur mineral content, specific surface area, temperature, and P_{CO_2}.

3 Results

3.1 Carbon mineralisation potential

Nearly all Earth MRI projects report at least some materials with $C_{pot} > 100$ (kg CO_2/tonne (t) of material; Figure 1). For this evaluation, a $C_{pot} > 100$ value has been selected as a reasonable threshold for carbon mineralisation potential. Therefore, samples with $C_{pot} < 100$ are deemed to have minimal or questionable potential while those with $C_{pot} > 100$ should be considered viable options for carbon mineralisation feedstock. The range of potential within a project—and across projects—highlights the need to identify unique materials (i.e., rocks) with the greatest potential.

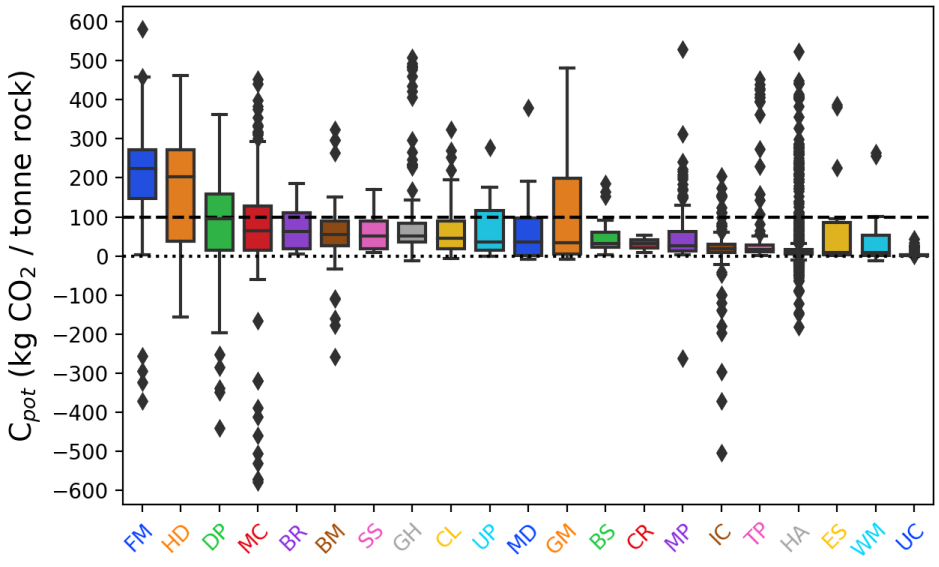

Figure 1 **Bulk C_{pot} for projects reported in the Earth MRI dataset presented in a box-and-whisker format. Centre lines denote P50 while the box edges denote IQR (difference between P25 and P75). The whiskers extend no greater than 1.5*IQR outside box edges. The dotted line indicated zero C_{pot} and the dashed line indicates C_{pot} = 100 kg CO_2/t. Most projects report some materials with C_{pot} > 100 kg CO_2/t**

Materials with median values greater than C_{pot} = 100 are reported in Table 3. The most common high-potential materials are basalts (including metabasalt and amphibolite) and gabbros (including metagabbro and gabbronorite). Basalts were identified in nine of the projects, whereas gabbros were present in six projects. Other high-potential materials that are present at multiple sites include lamprophyre (two) and pyroxenite (two). There are several other materials that occur at multiple sites; however, these materials are discounted by the authors. Breccia, sandstone, siltstone, claystone, and shale are likely to have pre-existing carbonate minerals. Other materials—like vein, igneous unidentified, and schist—are vague and difficult to interpret.

The IL-KY Fluorspar District-Midwest Ultramafic District (FM) and the Hicks Dome (HD) area show the greatest potential, both having median C_{pot} > 200. Lampophyres are abundant in both projects. Modal mineralogy data from these projects aren't available; however, it is possible the mineral phlogopite, commonly found in lamprophyres, contributes to the relatively high potentials (phlogopite C_{pot} = 316 kg CO_2/t; Table 2).

Ultimately, the ability to sequester large amounts of carbon requires more than the presence of high-potential materials; there must also be an abundance. Furthermore, these materials need to be subjected to activities that will increase surface area and subsequently be exposed to weathering to realize their potential. The upside to this requirement is that materials with modest potential could sequester large quantities of carbon when scaled to large waste rock and tailings disposal facilities at mining operations. Thus, through thoughtful material handling practices, materials with modest and high potential can be managed to encourage weathering and associated carbon mineralisation reactions, whereas minerals with low or negative potential can be isolated to discourage weathering.

Table 3 Carbon mineralisation potential (kg CO_2/t) organized by project

Project Name	Label	Median C_{pot}	Material with median C_{pot} > 100 kg/t, (#) = n
IL-KY Fluorspar Dist.; Midwest Ultramafic Dist.	FM	223	breccia (3), igneous unidentified (44), lamprophyre (86), shale (1)
Hicks Dome area, IL & KY	HD	203	sedimentary unidentified (1), lamprophyre (98), breccia (5)
Devonian Phosphatic Units, Appl. and IL Basins	DP	95	siltstone (4), nodule (27), shale (102)
Mentor Complex Region	MC	64	pyroxenite (2), schist (11), anorthosite (6), gabbro (9), metamorphic unidentified (1), basalt (12), dacite (6)
Blue Ridge area, MD	BR	64	metabasalt (3)
Bull Mountains-Elkhorn Mining Dist., MT	BM	54	lapilli (2)
Salton Sea Trough, CA	SS	51	basalt (1)
Gold Hill Mining Dist., UT	GH	51	sandstone (10), claystone (1), chert (1), quartz diorite (1)
Central Laramie Range, WY	CL	46	metamafic (1), hornfels (1), skarn (1), metasedimentary (3), amphibolite (1), troctolite (1), gabbro (2), mafic (6), quartzite (1), gabbronorite (6), gneiss (6)
Upper Peninsula, MI	UP	36	metagabbro (2), meta-ultramafic (1), basalt (3), amphibolite (2), gabbro (11), pyroxenite (2)
Marine phosphate deposits, AR	MD	35	-
Gallinas Mountains, C. NM	GM	35	fenite (1), breccia (11), vein (2), sandstone (52), tactite (3), volcanic breccia (4)
Big Sandy Valley, AZ	BS	32	diabase (1), basalt (2)
Clayton Valley, Rhyolite Ridge, W NV	CR	31	-
Mountain Pass area, CA & NV	MP	27	sinter (1), calcsilicate (1), monzonite (2), amphibolite (10), basalt (2), diorite (1)
ID cobalt belt	IC	19	gabbro (2)
Trans-Pecos Tertiary Alkaline Rocks, NM & TX	TP	17	vein (7), conglomerate (2), jasperoid (2), claystone (1)
High Alumina Underclay Deposits, Appalachian and Illinois Basins	HA	9	vein (4), kimberlite (8), igneous unidentified (48)
Eastern St. Francois Mountains, MO	ES	9	siltstone (2)
Wet Mountains, CO	WM	9	schist (1)
Upper Coastal Plain, SC	UC	2	-

3.2 Carbon mineralisation rates

A material's ability to sequester carbon via mineralisation depends on its bulk potential and reactivity. Characteristic dissolution rates determine whether significant amounts of carbon can be mineralized on relevant timescales. Modelling dissolution and subsequent carbon mineralisation processes based on published rate data may be problematic because (i) mineral dissolution databases do not always agree on dissolution rates and (ii) rate data collected on individual mineral phases poorly predict the reactivity of multi-phase aggregates (i.e., rocks).

To illustrate the opportunities and challenges involved in modelling carbon mineralisation rates, a model was used to dissolve a hypothetical mafic rock, thus releasing its carbon mineralisation potential over time as each constituent mineral was allowed to dissolve. Simulations were performed using three prominent databases of mineral dissolution rates *(Bullock et al., 2021; Heřmanská et al., 2022; Palandri and Kharaka, 2004)*. Results show broad agreement across rate compilations with respect to the timescale of C_{pot} release (Figure 2). However, there is disagreement over the relative importance of the three mineral components modelled.

The hypothetical material was assumed to be comprised of 20% forsterite (Mg_2SiO_4; Fo.), 40% enstatite ($MgSiO_3$; En.), and 40% anorthite ($CaAl_2Si_2O_8$; An.), with a bulk C_{pot} of 360 kg/t (about one-third of which is released on the timescale of a 100 years regardless of the rate compilation used). Following the approach of Bullock et al. (2021), mineral dissolution rates were calculated for circumneutral pH (assumptions around pH are explored in Section 3.3). All three simulations depict a slowing rate of C_{pot} release as the more reactive minerals become depleted. Forsterite is highly reactive in all three simulations, but the relative importance of anorthite depends on the rate compilation used. The reactivity of anorthite (and calcium-bearing feldspars in general) is important because these minerals are widely distributed at mine sites.

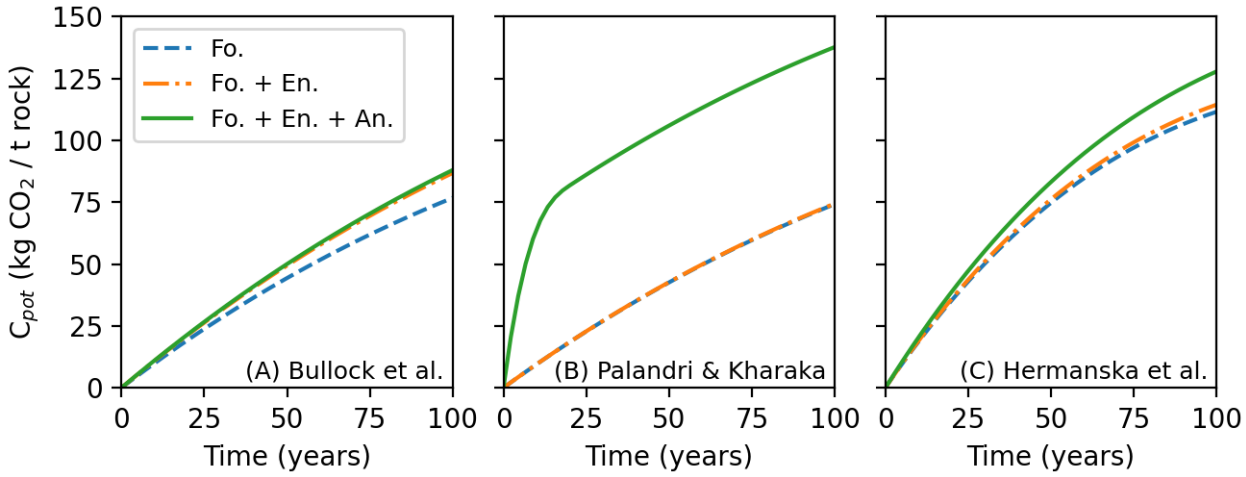

Figure 2 **Realized carbon mineralisation potential simulated over time for a 0.1 mm diameter material composed of 20% forsterite (Fo.), 40% enstatite (En.), and 40% anorthite (An.) to represent a mafic rock with a bulk C_{pot} of 360 kg CO_2/t. Surface area normalized release rates calculated at pH 7 from (A) Bullock et al. (2021) following Bandstra et al. (2008), (B) Palandri and Kharaka (2004), and (C) Heřmanská et al. (2022). Blue dashed curves show contribution of forsterite alone, orange dash-dot curves show the contribution of forsterite and enstatite combined, and the solid green line shows the contribution from all three minerals**

The contribution of anorthite can be visualized in Figure 2 by the separation between the Fo. + En. + An. curve and the Fo. + En. curve. Rates sourced from Bullock et al. (2021) suggest a negligible contribution from anorthite over a century-long time-scale while simulations based on Palandri and Kharaka (2004) suggest that anorthite reacts in only a few years. Simulations based on Heřmanská et al. (2022) predict an

intermediate rate for anorthite. Per Table 2, anorthite contributes 63 kg/t to the bulk C_{pot} of the mixture simulated in Figure 2 regardless of the release rate. However, for many mafic materials a much greater fraction of the bulk C_{pot} may be associated with calcium-bearing silicate minerals.

The rate data in the kinetics compilations used in Figure 2 are based on far-from-equilibrium dissolution rates for carefully prepared mineral separates. Comparing these simulations to an empirical model fitted to laboratory kinetic test data with mafic waste rock (Figure 3) suggests that far-from-equilibrium rates are a reasonable proxy for the overall rate of C_{pot} release even though the waste rock is more complex than a simple mixture of calcium- and magnesium-bearing silicates. The data-driven model results suggest that calcium release plays a greater role than would be predicted by rates from Bandstra et al. (2008) but a smaller role than would be predicted by Palandri and Kharaka (2004). The relative contributions of calcium and magnesium are well modelled by rates from Heřmanská et al. (2022) and these results suggest that materials with significant quantities of calcium-rich feldspar should be considered viable materials for carbon sequestration.

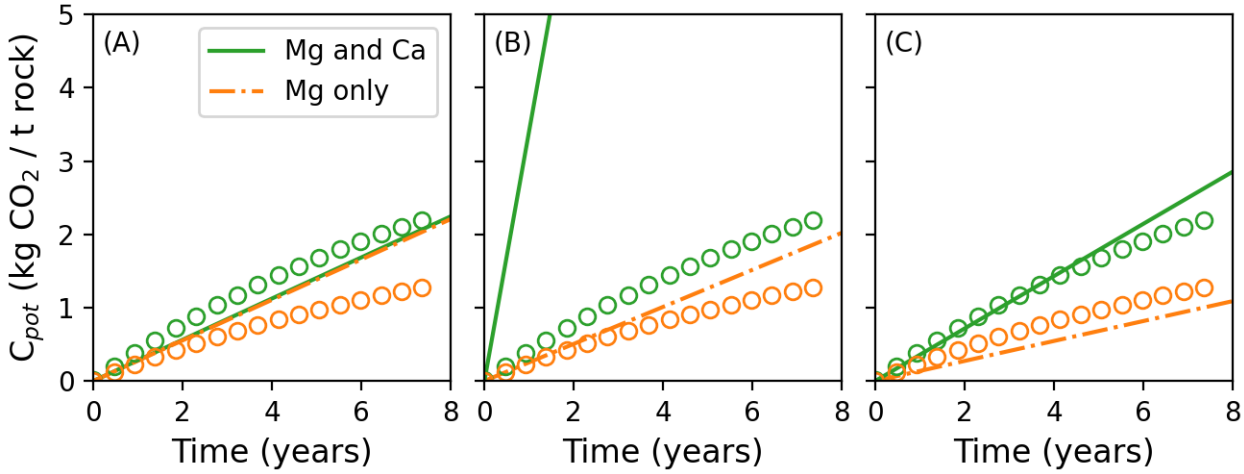

Figure 3 **Comparison of literature based C_{pot} release rates to results from a data-driven model. Literature-based results depicted as curves using rates from (A) Bullock et al. (2021), (B) Palandri and Kharaka (2004), and (C) Heřmanská et al. (2022), assuming geometric surface area of 0.4 mm particles and a Fo./En./An. mixture of 21/18/61 to match material used in kinetic testing. Data-driven results depicted as circles using fitted empirical rates from Bandstra et al. (In prep.). In all cases, magnesium contributions to C_{pot} are depicted in orange while the combined contributions from magnesium and calcium are depicted in green**

3.3 Conditions for carbonate precipitation

Dissolving the cations that constitute C_{pot} is only the first step in carbon mineralisation. To complete the process, the cations must then react with carbonate species to form mineral precipitates. This is illustrated by the reactions of magnesium and calcium to form hydromagnesite and monohydrocalcite, respectively:

$$4\,HCO_3^- + Mg^{+2} + 6\,H_2O = Mg_5(CO_3)_4(OH)_2(H_2O)_{4(s)} + 6H^+ \quad (4)$$

$$HCO_3^- + Ca^{+2} + H_2O = CaCO_3(H_2O)_{(s)} \quad (5)$$

The hydrated carbonate solids (products) in reactions (6) and (7) are metastable relative to reactants magnesite and calcite from a thermodynamic perspective. However, they are anticipated to be kinetically favourable during initial solid formation. In the precipitation simulations shown below, the carbonate solids are formed when sufficient magnesium, calcium, and bicarbonate are dissolved in solution to achieve thermodynamic saturation.

A batch-reactor simulation was developed to evaluate the rate of hydrated carbonate solid precipitation (from reactions (6) and (7); Figure 4A) and commensurate pH evolution, given variable sulphur content (all sulphur assumed to be pyrite, as percent sulphur or wt. %S; Figure 4B). Silicate reactivity for this simulation is the same as in Figure 3C. Pyrite content was modelled for 0.01, 0.1, and 1 wt. % S.

Simulation results (Figure 4) suggest that substantial quantities of carbonate solid can be formed on a timescale of years provided that the sulphide content of the mineral feedstock is low (i.e., less than 1%). Both magnesium- and calcium-bearing carbonates can form on a meaningful timescale, reinforcing the observation that calcium-bearing silicates can be used a feedstock for carbon mineralisation. Note, however, that although all of the hypothetical materials simulated in Figure 4 have positive C_{pot}, pyrite oxidation in the 1% S case lowers the pH to a point where reactions (6) and (7) cannot achieve saturation due to low levels of bicarbonate in solution. Figure 4B suggests that the threshold for mineral carbonation is around pH = 8.

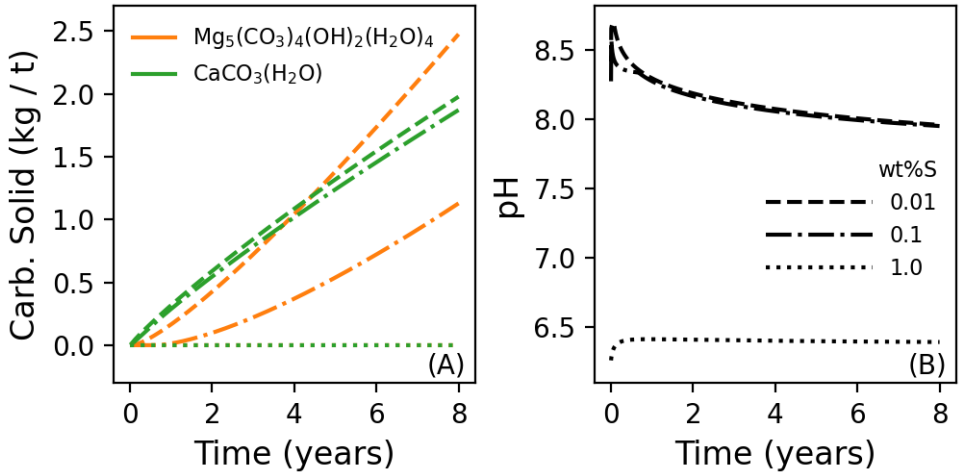

Figure 4 **Time series simulations of carbonate solid formed (A) and pH (B) in a batch reactor with silicate reactivity identical to Figure 3C and variable sulphur content (as pyrite). The line-styles in the legend of panel B are indicative of sulphur content in panel A**

3.4 Carbon mineralisation enhancements

An average carbonate formation rate can be derived from simulations like those shown in Figure 4 by taking the amount of solid formed at the simulation end and dividing by time. Precipitation rates for both hydromagnesite and monohydrocalcite can be aggregated by converting the mass of solid formed to equivalents of CO_2 consumed as:

$$Rate = \frac{\Delta M_{mag.}}{\Delta t} \cdot \frac{4\ mol\ CO_2}{1\ mol\ mag.} \cdot \frac{FW_{CO_2}}{FW_{mag.}} + \frac{\Delta M_{calc.}}{\Delta t} \cdot \frac{1\ mol\ CO_2}{1\ mol\ calc.} \cdot \frac{FW_{CO_2}}{FW_{calc.}} \quad (6)$$

where ΔM_x represents the change in mass of carbonate phase x (hydromagnesite or monohydrocalcite for mag. and calc., respectively), Δt represents the averaging time, and FW_x represents the formula weight of compound x. The average rate defined in equation (8) provides a ready means of comparing simulation results across factors that either enhance or detract from carbon mineralisation.

Figure 5 shows rates of carbon mineralisation as a function of sulphur content (as pyrite). All simulations shown reinforce the observation of a sulphur content cut-off above which carbonate solids do not form (0.3% S). This kinetics-based cut-off is significantly lower than what would be estimated based on bulk C_{pot} calculated from the mineral chemistry with equation (3).

The bulk C_{pot} computed from equation (3) for the same mix of silicates simulated in Figure 4, but with a variable amount of additional sulphur (as pyrite), yields positive carbon mineralisation potential for sulphur contents up to 15%. Consequently, materials with a sulphide content above the 0.3% kinetics-based cut-off

may have large bulk carbon mineralisation potential that would not be realized under industry-standard waste rock management practices. Given that mined materials often have sulphide contents greater than 0.3% S, development of an innovative process to allow for carbon mineralisation from materials with moderate levels of sulphide would open a much wider range of materials for utilization in carbon sequestration. To develop a process of this type, it is important to understand the factors that influence the relevant reaction kinetics.

Rates of both cation release and carbonate precipitation are sensitive to environmental factors. Such rate dependencies may be used to enhance the net rate of carbon mineralisation. Figure 5 shows average rate simulations under a similar set of assumptions as used in the simulations of Figure 4, but with varied particle size (i.e., surface area), temperature, and P_{CO_2}. Both particle size and temperature alter the precipitation rate without changing the sulphur content cut-off above which carbonates do not form. Adjustment of P_{CO_2} alters both the rate and the sulphur cut-off.

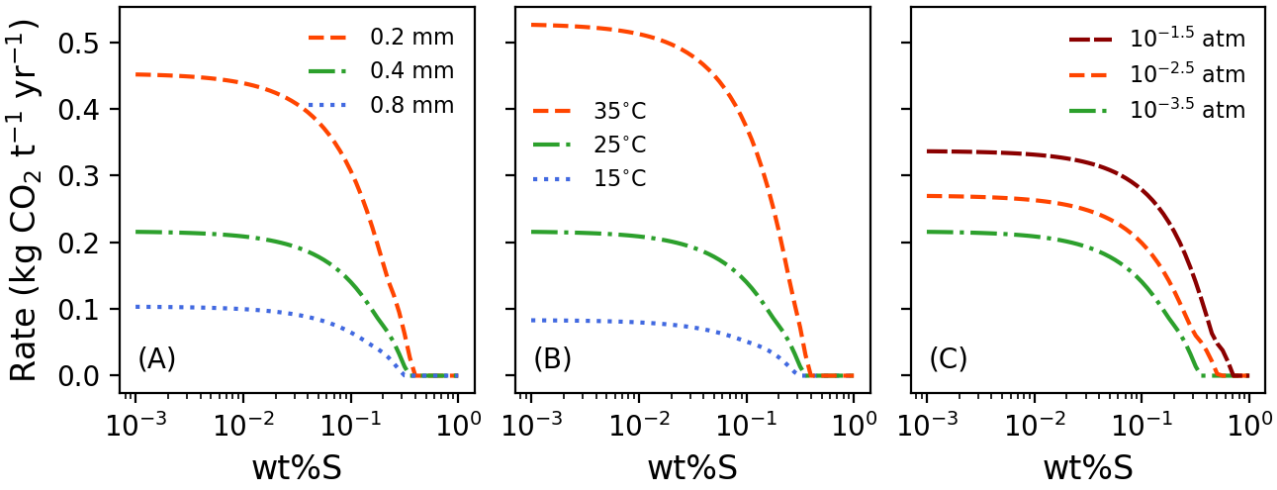

Figure 5 **Average rates of carbonate solid formation vs sulphur content with rate enhancements by particle size (A), temperature (B), and P_{CO_2} (C)**

Decreasing the particle size (Figure 5A) causes a proportionate increase in the specific surface area and rate of cation release. When the sulphide content is below the kinetics-based cut-off, carbonate solid precipitation is rate limited by cation release and therefore halving the particle diameter leads to doubling of the precipitation rate. Above the sulphide cut-off, carbonate solids cannot form under the passive conditions of a simple batch reactor and these conditions are not responsive to the surface area of the material.

Similar to surface area, increased temperature leads to increased reactivity of all dissolving minerals. Most environmentally relevant reactions have activation energies such that a 10° C increase in temperature leads to an approximate doubling of the reaction rate. The simulated response to temperature adjustment (Figure 5B) follows a similar pattern to particle size (Figure 5A).

The effect of CO_2 content (Figure 5C) is more complex than particle size or temperature. Increasing the P_{CO_2} causes a decrease in solution pH. This, in turn, leads to increased rates of silicate mineral dissolution and divalent cation release. While the decrease in pH due to increased sulphur content (see Figure 4) tends to prohibit carbonate solid formation, the same is not true when pH is decreased by dissolved CO_2. Increased P_{CO_2} raises the concentration of bicarbonate ions needed to drive precipitation reactions (6) and (7) and, consequently, the sulphur content cut-off for carbonate precipitation is elevated by enhanced CO_2.

Implementation of rate enhancements of the type described above represent a significant challenge particularly at the scale of a mine site. While a number of studies have developed engineered processes to enhance mineral-based carbon sequestration—e.g., Azdarpour et al. (2015), most do not adequately address

the large mass of material that would need to be handled (Kelemen et al., 2020). There is an urgent need for new research to develop methods of rate enhancement that account for the geotechnical constraints inherent in mine-waste management.

4 Conclusion

Mining projects provide a unique opportunity to enhance passive carbon mineralisation rates and sequester appreciable amounts of carbon on human timescales. Our results suggest carbon sequestration is more accessible to mining companies than current knowledge suggests. Of the 21 Earth MRI projects evaluated for bulk carbon mineralisation potential, 20 had samples with $C_{pot} > 100$ kg CO_2/t of material. In addition, dissolution rate data published by Heřmanská et al. (2022), which align with data-driven (i.e., site-specific) results from Bandstra et al. (In prep.), suggest rocks with calcium-bearing feldspars should be considered as potential feedstock targets for carbon mineralisation. Enhancements like grain size optimizations and the introduction of heat or additional CO_2 may improve mineralisation rates further. Innovative processes need to be developed to account for sulphide concentrations above the reported cut-off and broaden the range of materials used in carbon sequestration projects.

Acknowledgement

This work was funded by National Science Foundation (NSF) Small Business Innovative Research (SBIR) Phase II Award No. 2212919: Predictive Tools for Characterizing Carbon Sequestration in Mined Materials.

The authors gratefully acknowledge contributions from Rachel Gibson, Xiang Li, and Steph Theriault.

References

Azdarpour, A et al., 2015. A Review on Carbon Dioxide Mineral Carbonation through Ph-Swing Process. *Chemical Engineering Journal*, 279: 615-630.

Bandstra, J, Swenson, J, Haus, A, and Diedrich, T, In prep. Sulfide-Induced Silicate Weathering Can Enhance Carbon Mineralization in Plagioclase-Rich Mine Waste.

Bandstra, J Z et al., 2008. Appendix: Compilation of Mineral Dissolution Rates. In: Brantley, S.L., Kubicki, J.D., White, A.F. (Eds.), *Kinetics of Water-Rock Interaction*. Springer, New York.

Bullock, L A, James, R H, Matter, J, Renforth, P, and Teagle, D A H, 2021. Global Carbon Dioxide Removal Potential of Waste Materials from Metal and Diamond Mining. *Frontiers in Climate*, 3.

Charlton, S R, and Parkhurst, D L, 2011. Modules Based on the Geochemical Model Phreeqc for Use in Scripting and Programming Languages. *Computers & Geosciences*, 37(10): 1653-1663.

Gras, A, Beaudoin, G, Molson, J, and Plante, B, 2020. Atmospheric Carbon Sequestration in Ultramafic Mining Residues and Impacts on Leachate Water Chemistry at the Dumont Nickel Project, Quebec, Canada. *Chemical Geology*, 546(546).

Hamilton, J L et al., 2021. Carbon Accounting of Mined Landscapes, and Deployment of a Geochemical Treatment System for Enhanced Weathering at Woodsreef Chrysotile Mine, Nsw, Australia. *Journal of Geochemical Exploration*, 220.

Heřmanská, M, Voigt, M J, Marieni, C, Declercq, J, and Oelkers, E H, 2022. A Comprehensive and Internally Consistent Mineral Dissolution Rate Database: Part I: Primary Silicate Minerals and Glasses. *Chemical Geology*(597): 120807.

International Finance Corporation, 2023. Net Zero Roadmap Fot Copper and Nickel, Technical Report.

Kelemen, P B et al., 2020. Engineered Carbon Mineralization in Ultramafic Rocks for Co2 Removal from Air: Review and New Insights. *Chemical Geology*, 550.

Kularatne, K, Sissmann, O, Guyot, F, and Martinez, I, 2023. Mineral Carbonation of New Caledonian Ultramafic Mine Slag: Effect of Glass and Secondary Silicates on the Carbonation Yield. *Chemical Geology*, 618.

Kuykendall, T, 2021. Path to Net-Zero: Drive to Lower Emissions Pays in Metals, Mining Sector, S&P Global Inc.

Lechat, K, Lemieux, J-M, Molson, J, Beaudoin, G, and Hébert, R, 2016. Field Evidence of Co 2 Sequestration by Mineral Carbonation in Ultramafic Milling Wastes, Thetford Mines, Canada. *International Journal of Greenhouse Gas Control*, 47: 110-121.

Palandri, J L, and Kharaka, Y K, 2004. A Compilation Fo Rate Parameters of Water-Mineral Interaction Kinetics for Application to Geochemical Modeling. U.S. Geological Survey. Open File Report 2004-1068. March 2004.

Parkhurst, D, and Appelo, C, 2013. Description of Input and Examples for Phreeqc Version 3–a Computer Program for Speciation, Batch-Reaction, One-Dimensional Transport, and Inverse Geochemical Calculations. *Book 6: Modeling Techniques*. U.S. Geological Survey. Chapter 43 of Section A, Groundwater.

Power, I M, Dipple, G M, Bradshaw, P M D, and Harrison, A L, 2020. Prospects for Co2 Mineralization and Enhanced Weathering of Ultramafic Mine Tailings from the Baptiste Nickel Deposit in British Columbia, Canada. *International Journal of Greenhouse Gas Control*, 94.

Power, I M et al., 2013. Carbon Mineralization: From Natural Analogues to Engineered Systems. *Reviews in Mineralogy and Geochemistry*, 77(1): 305-360.

Renforth, P, 2019. The Negative Emission Potential of Alkaline Materials. *Nature Communications*, 10(1): 1401.

Reynes, J F, Mercier, G, Blais, J-F, and Pasquier, L-C, 2021. Feasibility of a Mineral Carbonation Technique Using Iron-Silicate Mining Waste by Direct Flue Gas Co2 Capture and Cation Complexation Using 2,2′-Bipyridine. *Minerals*, 11(4).

Rimstidt, J D, 2014. *Geochemical Rate Models: An Introduction to Geochemical Kinetics*. Cambridge University Press, New York.

Steinour, H H, 1959. Some Effects of Carbon Dioxide on Mortars and Concrete-Discussion. *Journal of the American Concrete Institute*, 30(2): 905-907.

Wilson, S A et al., 2011. Subarctic Weathering of Mineral Wastes Provides a Sink for Atmospheric Co(2). *Environmental Science & Technology*, 45(18): 7727-36.

Wilson, S A et al., 2014. Offsetting of Co2 Emissions by Air Capture in Mine Tailings at the Mount Keith Nickel Mine, Western Australia: Rates, Controls and Prospects for Carbon Neutral Mining. *International Journal of Greenhouse Gas Control*, 25: 121-140.

Woodall, C M, Lu, X, Dipple, G, and Wilcox, J, 2021. Mineralization with North American Pgm Mine Tailings - Characterization and Reactivity Analysis. *Minerals*, 11(844).